

COMPARISONS OF BONE DENSITY MEASUREMENTS BETWEEN QUANTITATIVE COMPUTED TOMOGRAPHY AND MAGNETIC RESONANCE IDEAL IMAGING

K-Y. Ho¹, H. H. Hu¹, J. H. Keyak², P. M. Colletti¹, and C. M. Powers¹

¹University of Southern California, Los Angeles, California, United States, ²University of California, Irvine, California, United States

Introduction-Quantitative computed tomography (QCT) has been commonly used to acquire subject-specific, volumetric bone densities in vivo. With QCT, bone is modeled as a specimen composed of water and mineral, and the x-ray attenuation coefficients (i.e., Hounsfield number) after being corrected with scan phantoms, is used to calculate the mineral density of each voxel.[1] With QCT, a heterogeneous bone finite element (FE) model can be generated by assigning 3-dimensional density measures to FE bony mesh. However, as articular cartilage exhibits little signal on CT, such an approach becomes challenging when structuring cartilage contact problems (e.g., patellofemoral joint). As such, we utilize fat-water chemical shift imaging (IDEAL MRI) [2-3] to estimate bone density in vivo with the assistance of a calcium hydroxyapatite (CHA) calibration phantom. The assumption is that 1) bone consists of water, fat and mineral, and 2) bone mineral density is negatively associated with the porosity of bone (i.e., space occupied by water and fat molecules). Thus, bone densities are hypothesized to be negatively corrected with their in-phase (IP: water+fat) values acquired from IDEAL protocol. The purposes of this study are 1) to investigate the relationship between CHA densities and MR signal intensities, and 2) to correlate the bone density measurements between QCT and IDEAL.

Methods-Five 40ml phantoms with various mass of CHA (0 g, 4g, 8g, 12g, and 16g) and distilled water, which were equivalent to CHA density 0 g/ml, 0.1 g/ml, 0.2 g/ml, 0.3 g/ml, and 0.4 g/ml, were constituted for MR scan on a 3T GE scanner with a single-channel head coil. To examine the phantoms in a suspension state, a spoiled-gradient-echo pulse sequence (TR=10ms, TE=4.4ms, flip angle=5°, slice thickness=2 mm, FOV= 150*150 mm, matrix=128*128, NEX=12) was performed immediately after completely mixing CHA and water. As there was no fat in the CHA phantoms, TE was arbitrary. The image signal intensity of each CHA phantom was defined as average signal intensity within each phantom sample on 4 slices (Fig. 1). The signal intensities were plotted against the CHA densities and Pearson correlation coefficient was calculated.

The sample with CHA density 0.4g/ml was then utilized as a calibration phantom for quantifying CHA equivalent density in vivo during an IDEAL scan. A spoiled-gradient-echo IDEAL pulse sequence was performed on a female's knee joint (40 year, 1.67 m, and 57 kg) with an 8-element knee coil: TR= 20.2 ms, TE= {1.68 2.67 3.65 4.63 5.62 6.61} ms, slice thickness= 2 mm, FOV= 160*160 mm, matrix= 256*256, BW= 125 kHz. The CHA equivalent density (ρ_{CHA}) of each voxel within patella was calculated using the following equation from IDEAL reconstructed IP imaging (Fig. 2):

$$\rho_{CHA} \left(\frac{g}{ml} \right) = \left\{ 1 - \left[\frac{S - IP_{CHA}}{IP_{MAX} - IP_{CHA}} \right] \right\} \times 0.4$$

,where ρ_{CHA} is CHA equivalent density, S represents IP value, IP_{MAX} is maximum IP value at the subcutaneous fat region (Fig. 2-F), IP_{CHA} is IP value of CHA phantom (Fig. 2-G), and 0.4 g/ml is density of CHA phantom.

CT scan was obtained using a Siemens scanner with the following parameters: 80 kVp, 210 mA, 2-mm slices, 160*160 mm FOV, and 512*512 matrixes. Another set of CHA calibration phantom at concentrations of 0.15 g/ml, 0.075 g/ml, and 0 g/ml (Image Analysis, Columbia, KY) was used to calculate the CHA equivalent density on QCT imaging (Fig. 3). To compare IDEAL- and QCT-based density measures, the position of patella on QCT imaging was registered to its corresponding position on IDEAL IP imaging for each slice using a custom Matlab program (MathWorks, Inc.) (Fig. 4). After positional registration, the average CHA equivalent densities of every 4 pixels (1.25*1.25 mm) within the patella bone region on IDEAL IP and QCT imaging were calculated and evaluated with Pearson correlation coefficient. The significant level value was set as 0.05.

Results-An excellent linear correlation between CHA density and MR signal intensity was observed ($r=0.98$, $p=0.007$) (Fig. 5). The CHA equivalent densities calculated on IDEAL IP imaging were significantly correlated with those quantified from QCT on a human patella ($r=0.85$, slope=0.98, intercept= -0.15, $p<0.001$) (Fig. 6).

Discussion-With a CHA calibration marker, the current study has demonstrated that the IDEAL IP imaging can be used to quantify bone density in the patella. The linearity between CHA density and MR signal intensity has provided the support on our signal model for estimating CHA equivalent density. The differences in CHA equivalent density measurements between QCT and IDEAL were thought to be related to 1) different signal models utilized in 2 approaches, and 2) systemic errors resulting from positional registration. The subject-specific, volumetric bone density measurements acquired from IDEAL would provide an alternative approach for creating FE bone models. For instance, a heterogeneous patella FE model can be generated by assigning the material properties (function of density) [4-5] to the corresponding FE elements of patella geometry (Fig. 7). As only one subject was studied in this preliminary investigation, future efforts will focus on increasing the sample size to better understand the relationship between QCT- and IDEAL- based bone density measurements.

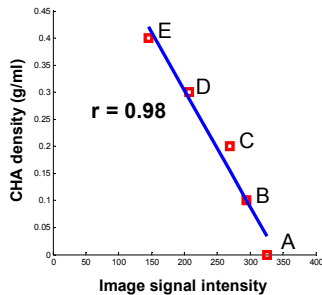


Fig. 5. Correlation between CHA densities and image signal intensities: A, B, C, D, E represent the CHA samples in Fig. 1.

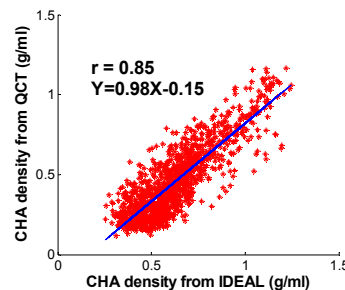


Fig. 6. Correlation between the CHA densities estimated from QCT and MR IDEAL protocol.

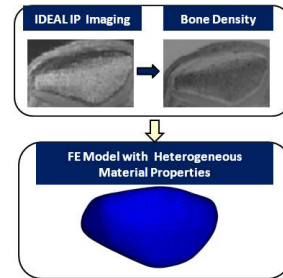


Fig. 7. The framework for generating a heterogeneous patella FE model according to the density measures on IDEAL IP imaging.

Reference-[1] Cann CE, *Radiology* 166: 509-522,1988. [2] Kijowski R, et al. *J Magn Reson Imaging* 29:436-442, 2009. [3] Reeder SB, et al. *J Magn Reson Imaging*. 25:644-652, 2007. [4] Carter DR and Hayes WC, *J Bone Joint Surg Am*. 59: 954-962, 1977. [5] Keyak JH, et al. *Clin Orthop Relat Res*. 437: 219-228, 2005.

Acknowledgement-The authors thank Sabafish Co., Ltd. for CHA material supply and GE Healthcare Applied Science Laboratory for technical support.